



X-ray photoelectron spectroscopy study of copper sodium silicate glass surfaces

A. Mekki^{a,b}, D. Holland^{a,*}, C.F. McConville^a

^a Department of Physics, University of Warwick, Coventry, CV4 7AL, UK

^b Department of Physics, KFUPM, Dhahran, 31261, Saudi Arabia

Received 9 September 1996; revised 27 January 1997

Abstract

Copper oxide-containing, sodium silicate glasses with composition $(0.70 - x)\text{SiO}_2 - 0.30\text{Na}_2\text{O} - x\text{CuO}$ (x in the range 0–0.2), were prepared by conventional melting and casting. The surface structure has been investigated by X-ray photoelectron spectroscopy. Evidence for the presence of copper in the Cu^+ state for glasses with $x \leq 0.14$, and for both oxidation states (Cu^+ and Cu^{2+}) in the glass where $x = 0.18$, has been obtained from the “shake up” satellite structure of the Cu 2p core level spectra. A deconvolution procedure has been undertaken to determine quantitatively the $[\text{Cu}^{2+}]/[\text{Cu}_{\text{total}}]$ ratio. The non-bridging oxygen content, obtained from the deconvolution of the O 1s core level spectra, increases with increasing copper oxide content indicating that copper acts as a network modifier. The O 1s spectra were modelled in such a way as to separate the contributions from SiOCu and SiONa to the non-bridging oxygen signal. © 1997 Elsevier Science B.V.

1. Introduction

The importance of copper and copper oxide based compounds in such diverse fields as catalysts [1–3] and high temperature superconductors [4,5] has increased in recent years. In particular, one of the most common questions raised concerns the chemical state of the copper atoms in these materials, i.e., to what extent is monovalent, divalent, or trivalent Cu observed. Core-level X-ray photoelectron spectroscopy (XPS) can provide information about the chemical state of a given atom by measuring the chemical shift associated with an appropriate core level for the atoms in different bonding configurations [6]. This chemical shift is a reflection of the change of the binding energy of core electrons with changes in the chemical environment. XPS has proved to be extremely useful in the study of copper oxide in catalysts [7–9], high temperature superconductors [10–14] and several polycrystalline compounds [15,16]. In addition, XPS has also been used in the study of alkali glasses of silicates [17–19], germanates [17,18] and phosphates [20] as well as more complex glass systems [21,22] (for example alkali aluminosilicate glasses). Despite this interest, to our knowledge there is little published work on the use of XPS in the study of the surface structure of oxide glasses containing elements from the first transition

* Corresponding author. Tel.: +44-1203 523 396; fax: +44-1203 692 016; e-mail: phsay@csv.warwick.ac.uk.

series. The bulk structure of transition metal oxide glasses has been studied extensively because of the interesting and diverse electrical [23,24] and magnetic properties [25] which they have as a consequence of their variable valence states [26]. Recently, however, XPS has been used to determine the valence states of iron in phosphates [27], and sodium silicate glasses [28], where a quantitative determination of ferric and ferrous ions was obtained from the fitting of the Fe 3p photoemission core level spectra by the contribution of Fe^{2+} and Fe^{3+} ions.

In the present paper, core level photoemission studies have been performed on a series of sodium silicate glasses, doped with various amounts of copper oxide, in order to determine the valence state of copper and the contribution of non-bridging oxygen atoms in these glasses.

2. Experimental procedure

2.1. Sample preparation

The glass samples were prepared using commercially available, analytical grade powders of CuO , Na_2CO_3 (for Na_2O) and SiO_2 . Calculated amounts of these powders were mixed and melted in 95%Pt/5%Rh crucibles at 1400°C for 2 h. The subsequent samples, obtained by quenching of the melt into deionized water, were crushed and remelted at the same temperature to ensure homogeneity of the product. This liquid was then cast into preshaped, graphite-coated steel moulds yielding bar specimens with dimensions $6 \times 6 \times 30 \text{ mm}^3$. After casting, the specimens were transferred to another furnace maintained at 50°C below the glass transition temperature, T_g , determined from differential thermal analysis (DTA), for 2 h and then cooled to room temperature at a rate of $30^\circ\text{C}/\text{h}$. X-ray powder diffraction analysis indicated that the samples thus formed were amorphous within the detection limit of the technique. After preparation, the samples were stored in a desiccator.

Chemical compositions were determined by inductively-coupled-plasma, emission spectroscopy (ICP). Each composition was analyzed at least twice and the estimated relative uncertainty in the composition derived from this technique was estimated to be $\pm 5\%$. Table 1 lists the batch and the analyzed glass compositions.

2.2. XPS measurements

These experiments were carried out in a spectrometer (V.G. Scientific ESCALAB MkII) equipped with a dual aluminum–magnesium anode X-ray source and a 150 mm concentric hemispherical analyzer. Photoelectron spectra from the C 1s, O 1s, Cu 2p, Na 1s and Si 2p core levels were recorded using a computer-controlled data collection system described elsewhere [29]. X-ray photoemission measurements were performed using non-monochromatic Al $K\alpha$ (1486.6 eV) radiation from an anode operated at 130 W. The energy scale of the

Table 1

Compositions of the as-prepared and analyzed copper sodium silicate glasses. The relative uncertainty in the ICP data is about $\pm 5\%$

x	Nominal			Analysed		
	Na_2O	SiO_2	CuO	Na_2O	SiO_2	CuO
0.0	0.30	0.70	0.0	0.31	0.69	0.0
0.04	0.30	0.65	0.05	0.30	0.66	0.04
0.09	0.30	0.60	0.10	0.30	0.61	0.09
0.14	0.30	0.55	0.15	0.30	0.56	0.14
0.18	0.30	0.50	0.20	0.30	0.52	0.18

spectrometer was calibrated using the Cu $2p_{3/2}$ = 932.67 eV, Cu $3p_{3/2}$ = 74.9 eV and Au $4f_{7/2}$ = 83.98 eV photoelectron lines [30]. The electron energy analyzer was operated with a pass energy of 10 eV for the high resolution XPS study (the analyzer energy resolution is 0.9 eV), whereas a pass energy of 50 eV was used for routine survey scans (not shown).

For XPS measurements, a glass rod from each composition was subsequently fractured in ultra high vacuum (UHV), where the base pressure in the analysis chamber was less than 2×10^{-10} mbar. The glass bars were notched to guide the fracture yielding flat, uncontaminated surfaces. Fracturing in UHV is regarded as the optimum method of producing a glass surface most representative of the bulk structure. Any other surface treatment (such as ion bombardment) may cause changes in surface composition and chemical state of the glass, especially the alkali ion distribution [31]. A period of approximately 2 h was required to collect the necessary data set for each sample and during this time, there was no evidence of any X-ray induced reduction of the copper, i.e., there was no change in chemical shift or peak shape for the Cu or O spectra. For consistency, all binding energies are reported with reference to the C 1s transition at $284.6 \text{ eV} \pm 0.2 \text{ eV}$. This peak arises from a minor quantity of hydrocarbon contaminants present in the vacuum and is generally accepted to be independent of the chemical state of the sample under investigation.

All of the spectra presented in this paper have been corrected for charging effects and the presence of any inelastic background. The O 1s and Cu 2p spectra were smoothed and fitted with the weighted sum of two Gaussian–Lorentzian curves (G–L ratio = 30%) representing the bridging and non-bridging oxygen contributions, and the possible copper valencies, respectively. The Lorentzian component of the fitted spectrum arises from the natural peak shape, while the Gaussian component represents the instrumental broadening contribution to the spectrum. Since the relative contributions are instrument dependent, the appropriate weighting was established by fitting a simple peak, such as C 1s, Si 2p or Na 1s, with the G–L ratio as one of the variables. This ratio was then kept constant when fitting the remaining spectra reported here. A non-linear, least squares algorithm was used to find each best fit solution. The bridging:non-bridging and $\text{Cu}^+:\text{Cu}^{2+}$ ratios were determined from the ratio of the areas under the respective peaks. Several samples were analyzed in this manner and the overall reproducibility in determining the peak position and chemical shift was $\leq 0.2 \text{ eV}$. The quantitative oxygen bonding results and copper redox analysis were reproducible to $\pm 5\%$ and $\pm 10\%$, respectively.

2.3. Glass properties

Several properties of each glass sample were measured. Glass transition temperatures were measured using DTA, and thermal expansion coefficients (α) were determined in the temperature range of room temperature to 400°C using dilatometry. The thermal expansion coefficient was measured relative to that of silica and a correction factor applied [32]. The density of each glass was also measured using Archimedes' principle and each sample was weighed both in air and in degassed, distilled water.

3. Results

3.1. C 1s spectra

In addition to the photoelectron and Auger transitions of the glass constituents, a weak C 1s transition was also observed. A high resolution spectrum near the C 1s region was recorded for each glass and revealed a weak single peak in the binding energy range 280 to 300 eV. This transition originates from background hydrocarbons in the vacuum system and this level has been used as an energy reference.

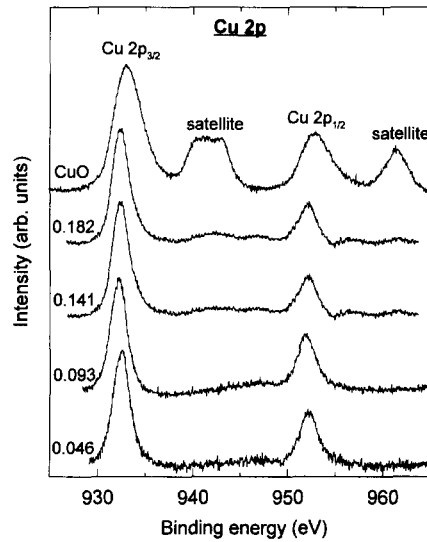


Fig. 1. High resolution core level spectra of the Cu 2p transition for the analyzed glass samples. A Cu 2p spectrum for the CuO powder sample is shown for comparison.

3.2. Cu 2p spectra

The core-level spectra in the region of the Cu 2p region are shown in Fig. 1 for the copper doped samples and for the pure CuO powder used in forming the glass samples. The peaks at binding energies of about 932.5 eV and 952.5 eV are due to the spin-orbit doublet of the Cu 2p core level transition. For the pure copper oxide powder, a strong satellite peak centered around 942 eV is observed, about 9 eV above the main core level line. For the sample with $x = 0.18$, a satellite above the main Cu 2p_{3/2} and Cu 2p_{1/2} photoelectron lines was also observed, although less intense than for the pure CuO. This feature is even less intense for the sample with $x = 0.14$ and absent from the spectra for samples with $x = 0.05$ and 0.09. This compares with the data of Frost et al. [33], who carried out a detailed study of over forty different copper compounds which showed that the

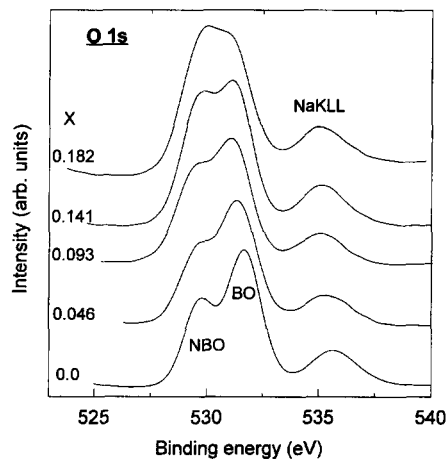


Fig. 2. High resolution core level spectra of the O 1s transition for the analyzed glass samples.

Table 2

Core-level binding energies (BE) of Na 1s, Si 2p and Cu 2p spectra, the uncertainty in the measured values is ± 0.2 eV. The numbers in parentheses represent the full width at half maximum

x	Na 1s BE (eV)	Si 2p BE (eV)	Cu 2p _{3/2} BE (eV)	Cu 2p _{1/2} BE (eV)
0.0	1071.5 (2.0)	102.0 (2.0)	–	–
0.05	1071.0 (2.4)	101.9 (2.3)	932.4 (2.1)	952.2 (2.1)
0.09	1070.8 (2.4)	101.6 (2.3)	932.3 (2.1)	952.1 (2.1)
0.14	1070.8 (2.4)	101.5 (2.3)	932.3 (2.1)	952.4 (2.1)
0.18	1070.9 (2.4)	101.4 (2.3)	932.5 (2.3)	952.3 (2.1)
CuO			933 (2.5)	952.9 (2.5)

width of the Cu 2p_{3/2} peak in all cuprous compounds is less than in cupric compounds. It can be seen from Fig. 1 (and Table 2) that the Cu 2p_{3/2} line widths for glass samples are less than those for CuO powder although there is an increase in the width of the line in the spectrum from the $x = 0.18$ sample. No changes in the binding energies of the Cu 2p core level peaks, greater than the errors in measurement, were observed in the samples as a function of x .

3.3. O 1s spectra

There are significant, compositionally dependent changes in the O 1s spectra of the samples shown in Fig. 2. Previous studies have established that the larger binding energy peak (~ 532 eV) in the spectrum of the 0.70SiO₂–0.30Na₂O base sample is due to bridging oxygen which is covalently bound to two silicon atoms (SiOSi), and the smaller binding energy peak (~ 529 eV) is due to non-bridging oxygen which is covalently bound to one silicon and ionically bound to one sodium (SiONa) [17,18]. The third peak at a binding energy at about 536 eV is attributed to the sodium KL₁L₂₃ Auger transition, obtained by creating the initial state hole with an X-ray instead of an electron. With increasing CuO content, the non-bridging contribution increases relative to the bridging oxygen component. It should be noted that the intensity of the sodium Auger transition is not affected by the change in copper content indicating that the sodium content in the near surface region of the glass remained approximately constant for all the samples investigated.

3.4. Si and Na core level spectra

XPS photoemission core level spectra for the remaining elemental constituents in the glass were also measured. The Si 2p and Na 1s spectra both showed symmetric peaks whose position varied only slightly as a function of copper content. These changes are summarized in Table 2 although the spectra are not shown here. As can be seen, the Si 2p peak position shifts to smaller binding energies by a total of about 0.7 eV, as the copper content is increased in the base glass. Similar behaviour has also been seen when increasing amounts of iron are incorporated into sodium silicate glasses [28].

Table 3

Variation of the density and glass transition temperature in (0.70 – x)SiO₂–0.30Na₂O– x CuO glasses

x	$\rho \pm 0.005$ (g/cm ³) at 20°C	$T_g \pm 1$ (°C)
0.0	2.406	475
0.042	2.407	417
0.09	2.534	371
0.14	2.651	353
0.18	2.865	348

Table 4
Variation of thermal expansion in $(0.70 - x)\text{SiO}_2 - 0.30\text{Na}_2\text{O} - x\text{CuO}$ glasses

x	Temperature (°C)	$\alpha \times 10^7 \pm 1$ (°C ⁻¹)
0.0	RT–350	147
0.05	RT–250	120
	250–350	156
0.09	RT–250	140
	250–350	159
0.14	RT–250	153
	250–350	185
0.18	RT–250	112
	250–350	149

After an initial shift of 0.4 eV, the Na 1s peak is not sensitive to changes in the copper oxide content of the base glass. The Na 1s peaks all have the same full width at half maximum (FWHM) of about 2.4 eV over the glass composition range investigated, suggesting that sodium exists in only one bonding configuration.

3.5. Physical properties

The glass transition and density measurements are reported in Table 3. The glass transition temperature decreases and the density increases with increasing copper content in the glass samples. The thermal expansion curve (change in length versus temperature) was non-linear over the temperature range of the measurements, for all the copper doped samples. The thermal expansion coefficient, α , for each sample is also shown in Table 4 as a function of x and temperature. For the temperature range room temperature to 250°C and $x \geq 0.0$, α increases until $x = 0.14$, then decreases slightly. A similar trend is also observed for α in the temperature range 250–350°C.

4. Discussion

4.1. Cu 2p spectra

The reported binding energy for the Cu 2p_{3/2} photoelectron core level in Cu₂O and in CuO polycrystalline compounds is 932.6 eV and 933.5 eV respectively [16,34]. Furthermore, it is also known that copper compounds containing Cu²⁺ ions are associated with strong satellites in the spectra, with binding energies at about 6 to 10 eV above the main core level lines, which are absent in compounds containing only Cu⁺ ions [16]. These satellites have been attributed to shake-up transitions by ligand-to-metal 3d charge transfer [35,36]. This charge transfer can occur for copper present in the Cu²⁺ form (3d⁹ configuration), however, it cannot take place if the copper is metallic or in the Cu⁺ state (3d¹⁰ configuration) due to the presence of a completely filled 3d shell. It is therefore possible to distinguish qualitatively between the two oxidation states of copper by recording the Cu 2p photoemission lines.

For $x = 0.05$ and 0.09 samples, no satellite structure was observed above the Cu 2p_{3/2} peak, indicating that the only valence state of copper in these two samples is Cu(I). If Cu(II) is present in these glass samples, then the amount is too small to be detected by XPS. For the $x = 0.14$ and 0.18 samples, there is a weak satellite at a binding energy ~ 9 eV greater than the main Cu 2p_{3/2} peak, indicating that both Cu(I) and Cu(II) coexist in these glass samples although, since the intensity of the satellite is very small compared to that observed in CuO, the amount of Cu(II) is expected to be small. As can be seen from Fig. 1, the intensity of the satellite for the $x = 0.14$ sample is less than for the $x = 0.18$ sample. Furthermore, the Cu 2p_{3/2} peak width for the $x \leq 0.14$

samples is also smaller than that of the $x = 0.18$ sample (Table 2), and the Cu 2p binding energies of these three samples agree well with previously reported values for compounds containing Cu(I) [34].

In order to determine ratios of the valence states of copper in these glasses, it was necessary to analyze the Cu 2p_{3/2} transition in relation to the copper content in the glass network. Monovalent and divalent copper are the only oxidation states observed in glass structures [26]. Therefore, each Cu 2p_{3/2} peak was resolved into two separate components, first being the contribution from Cu(I) and the second from the Cu(II), with the formal charge difference between Cu⁺ and Cu²⁺ reflected in the energy shift between the two transitions. The addition of valence electrons ('increasing electron density') effectively screens the core electrons and so decreases their measured binding energies. Therefore, the Cu⁺ should have a smaller binding energy than the Cu²⁺ contribution to the spectrum. Each component peak in the spectrum was fitted to a weighted sum of Gaussian–Lorentzian (G–L ratio = 30%) peaks, corresponding to Cu⁺ and Cu²⁺, by means of a least-squares fitting program [37]. For samples with $0.05 \leq x \leq 0.14$, it was not possible to fit the spectrum with two peaks, as initially expected. One peak was used to fit the Cu 2p_{3/2} spectrum in these glasses (e.g., Fig. 3a for the $x = 0.05$ sample). The absence (or very small intensity) of the satellite structure (fingerprint for the existence of Cu(II)) and the binding energy of the transition at 932.5 eV confirms that copper is only present as Cu(I) in these glasses. For the $x = 0.18$ sample, the Cu 2p_{3/2} peak was fitted with two contributions as shown in Fig. 3b. The higher binding energy peak was due to Cu²⁺ as discussed earlier. The results of the best peak fit to the experimental data are; Cu(I) = 89.7% and Cu(II) = 10.3%. Even though a very weak satellite is seen in the $x = 0.14$ sample, indicating some Cu(II) it was not possible to fit two distinct peaks in the Cu 2p spectrum of this sample.

4.2. O 1s spectra

The O 1s spectra shown in Fig. 2 are similar to those of Smets and Krol [38] who investigated the $(80 - x)\text{SiO}_2 - 20\text{Na}_2\text{O} - x\text{Tl}_2\text{O}$ glass. From the O 1s peak fitted with two contributions, they found good

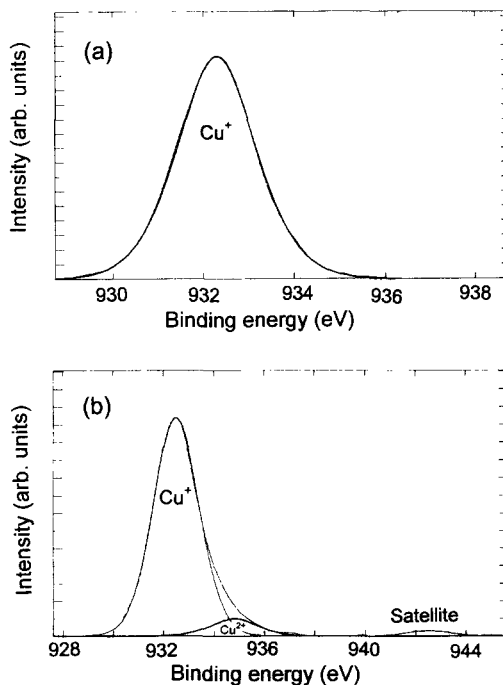


Fig. 3. (a) Cu 2p_{3/2} spectrum for the $x = 0.05$ glass fitted with a contribution from Cu⁺ ions only. (b) Cu 2p_{3/2} spectrum for the $x = 0.18$ glass fitted with contributions from Cu⁺ and Cu²⁺ ions.

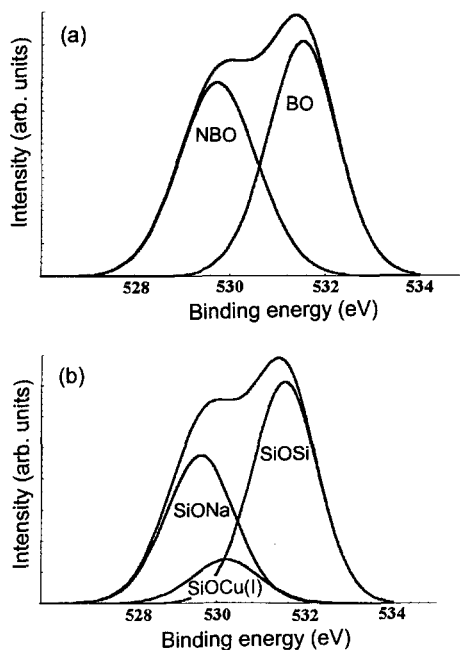


Fig. 4. (a) A two peak fit of the O 1s spectrum for the $x = 0.09$ glass. (b) Simulation of the O 1s spectrum for the same glass composition, showing all possible contributions to the O 1s transition.

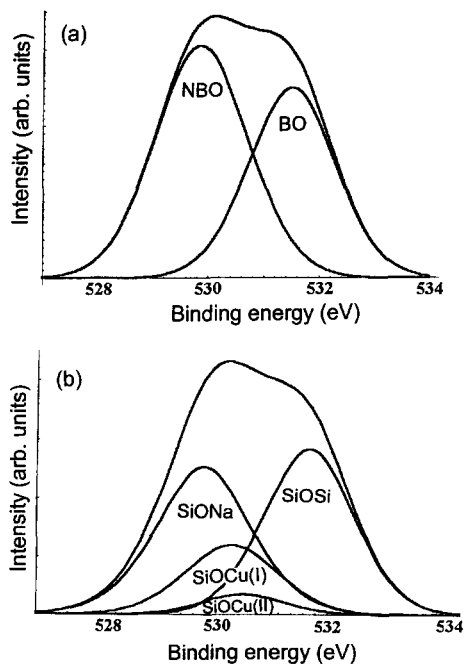


Fig. 5. (a) A two peak fit of the O 1s spectrum for the $x = 0.18$ glass. (b) Simulation of the O 1s spectrum for the same glass composition, showing all possible contributions to the O 1s transition.

agreement between the measured non-bridging oxygen to total oxygen ratio and the value calculated if the incorporated thallium was to behave as a monovalent modifier. A similar deconvolution method was also adopted for the O 1s spectra, and is shown in Figs. 4 and 5. The O 1s spectra were assumed to be composed of two overlapping peaks, and the best fit to the data for each composition was found by varying the peak position, width and intensity for each of the two components. The non-bridging to total oxygen ratio was determined from the area ratios (area of NBO/area of total oxygen). Fig. 4a Fig. 5a show the fitting of the O 1s spectrum, with contributions from BO and NBO, for $x = 0.14$ and $x = 0.18$ samples. As can be seen, the sum of two Gaussian–Lorentzian functions provides a good fit to the experimental data. The results of fitting the experimental O 1s spectra for $0.0 \leq x \leq 0.18$ are shown in Table 5. Previous studies have established that the experimental ratio of non-bridging to total oxygen in a $0.70\text{SiO}_2\text{--}0.30\text{Na}_2\text{O}$ glass is 38% in excellent agreement with our findings.

If the copper atoms in the glass do indeed behave as network modifiers, for each Cu_2O molecule (when $x \leq 0.14$) and CuO (when $x = 0.18$) that is added, two non-bridging oxygen atoms must be formed in the glass. Consequently, the fraction of non-bridging oxygen atoms should be given by

$$\text{NBO/Total oxygen} \begin{cases} = \frac{2[\text{Na}_2\text{O}] + 2[\text{Cu}_2\text{O}]}{[\text{Na}_2\text{O}] + 2[\text{SiO}_2] + [\text{Cu}_2\text{O}]} & \text{for } (x \leq 0.14) \\ = \frac{2[\text{Na}_2\text{O}] + 2[\text{CuO}] + 2[\text{Cu}_2\text{O}]}{[\text{Na}_2\text{O}] + 2[\text{SiO}_2] + [\text{CuO}] + [\text{Cu}_2\text{O}]} & \text{for } (x = 0.18) \end{cases}, \quad (1)$$

where the terms in brackets indicate concentrations.

There is good agreement between the above equations and the measured proportions of non-bridging oxygen atoms as seen from Table 3, showing that the O 1s signal from both SiOCu(I) (for $x \leq 0.14$) and SiOCu(I) plus SiOCu(II) (for $x = 0.18$) contribute to the non-bridging oxygen signal.

The changes in fitting parameters for the O 1s transitions, as CuO is substituted for SiO_2 in these glasses, are summarized in Fig. 6. The addition of CuO to the base glass results in a decrease in binding energy difference (ΔE) between the bridging and the non-bridging oxygen atoms indicating that the difference in chemical environment between them becomes smaller. However, this variation is not as large as when Fe_2O_3 is introduced into the same base glass $70\text{SiO}_2\text{--}30\text{Na}_2\text{O}$ [28]. This difference is possibly due to the fact that the Cu(I)–O bond is not as covalent as the Fe(III)–O bond and therefore the binding energy of the O 1s in the unit SiOCu(I) is closer to that of the O 1s in SiONa , while the binding energy of O 1s in the unit SiOFe(III) is closer to SiOSi than to SiONa . The full width at half maximum of the non-bridging oxygen peak increases, while that of the bridging oxygen does not show any compositional dependence. These changes probably reflect the increase in non-bridging oxygen sites with SiOCu(I) contributing to the non-bridging oxygen signal. The present level of instrumental resolution does not allow us to deconvolute the non-bridging oxygen signal into contributions from SiONa and SiOCu(I) because the binding energy difference between these two contributions is too small. However, a simulation can be carried out to separate and model those two components.

Table 5

Comparison between the measured and the predicted (from Eq. (1)) non-bridging to total oxygen ratio as a function of copper content in the glass

x	NBO/OT (%) measured	NBO/OT (%) calculated
0.0	38	35.3
0.05	39.2	38.8
0.09	45.6	44
0.14	52.9	50
0.18	58.3	55.1

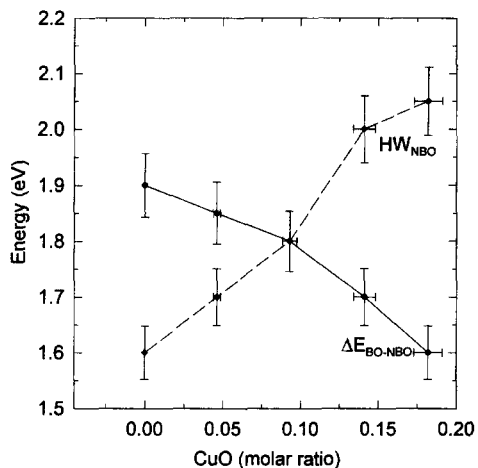


Fig. 6. Variation of the fitting parameters for the O 1s spectra versus CuO content in the glass. HW_{NBO} is the full width at half maximum of the non-bridging oxygen signal, while ΔE_{BO-NBO} is the separation between bridging oxygen and non-bridging oxygen transitions. Lines are drawn as guides for the eye.

Combinations of peaks were used to model independently the experimental spectra based on the chemical components present in the glass (note this is not the same as curve fitting, as in the case of the O 1s, when two components, BO and NBO, were used to *fit* the core level spectrum). This method was used to simulate the contributions from SiONa, SiOCu(I) and SiOCu(II) to the non-bridging oxygen signal [28]. In this method, the ratio Z/r for the ions bonded to the oxygens, was used as an approximate measure of their ability to remove charge from the oxygen and thus increase the O 1s binding energy. Z is the nominal charge on the ion and r is the radius of the ion in nanometers, thus giving Z/r of Si^{4+} (100), Na^+ (9.8), Cu^+ (21.74) and Cu^{2+} (27.40). These numbers can be used to derive values for the O 1s binding energies of the SiOCu(I) and SiOCu(II) configurations by linear interpolation between the observed values for SiOSi and SiONa (from the base glass). This method predicts that, as copper oxide is substituted for SiO_2 , the O 1s signal from SiOSi at 531.5 eV would gradually be replaced by peaks for SiOCu(I) and SiOCu(II) at binding energies of approximately 530.1 eV and 530.2 eV, respectively, while the SiONa peak would remain at 529.6 eV. Fig. 4b and 5b show the simulations based on the above model, using Gaussian–Lorentzian functions. In both cases the half widths were fixed at the values taken from the base glass sample and the intensities obtained from the chemical composition and the Cu^+/Cu^{2+} ratios calculated from the XPS data. The simulations shown in Fig. 4b and 5b are for the base glass doped with 9.3% and 18.2% CuO, respectively. It is clear that this simple model reproduces the experimental data for the glass samples shown with a high degree of accuracy. The same was also true for the compositions not shown here. It was, therefore, possible, from the XPS data and modelling, to separate all the possible contributions to the non-bridging oxygen signal.

4.3. Si 2p and Na 1s spectra

The shift to smaller binding energy for the Si 2p core level, shown in Table 2, was also observed in our previous study of iron sodium silicate glasses [28] and had previously been observed by Veal et al. in the study of sodium calcium silicate glasses [39]. This shift indicates an increase in the number of silicon atoms bonded to non-bridging oxygen atoms. In addition, we expect no direct bonding of copper with sodium in the glass and, therefore, only a minor fluctuation in the charge density on the sodium. This fluctuation is detected in the observation of only a small change in the overall binding energy of the Na 1s transition and no change in the line shape with increasing copper substitution.

4.4. Physical properties

The variation in the density, as copper is substituted for silicon in the glass, is expected because the density of copper oxide ($\sim 6.4 \text{ g/cm}^3$) is higher than that of silicon oxide ($\sim 2.65 \text{ g/cm}^3$). The glass transition on the other hand decreases with increase of copper content. The observed trends in the glass transition temperature and the thermal expansion coefficient would suggest that Cu(I) is indeed entering the glass as a modifying ion.

5. Conclusion

In the $(0.70 - x)\text{SiO}_2 - 0.30\text{Na}_2\text{O} - x\text{CuO}$ glass series with $0.0 \leq x \leq 0.18$, copper exists in only the Cu(I) state for samples with $x \leq 0.14$. For the sample with $x = 0.18$, the concentrations of Cu^+ and Cu^{2+} can be calculated by fitting the Cu $2p_{3/2}$ spectrum to contributions from both Cu(I) and Cu(II), giving values of 89.7% and 10.3% respectively. The ratios of non-bridging to total oxygen atoms, obtained by fitting the O 1s spectra, agree well with the values calculated from the glass composition if Cu(I) and Cu(II) behave as glass modifiers. The physical properties of the glasses presented in this paper, also indicate that copper ions are occupying modifying sites in the glass network. Using a simple model, based on the chemistry of the glass samples, we were able to simulate the non-bridging oxygen signal with contributions from SiONa, SiOCu(I) and SiOCu(II).

Acknowledgements

One of us (A.M.) would like to acknowledge the support of King Fahd University of Petroleum and Minerals (KFUPM) and the Physics Department of KFUPM.

References

- [1] C.N. Satterfield, *Heterogeneous Catalysis in Practice* (McGraw-Hill, London, 1980).
- [2] S. Matar, M.J. Mirbach, H.A. Tayim, *Catalysis in Petrochemical Processes* (Kluwer Academic, Dordrecht, 1989).
- [3] R.B. Anderson, in: *Catalysis*, Vol. 4, ed. P.H. Emmett (Reinhold, New York, 1956).
- [4] J.G. Bednorz, K.A. Muller, *Z. Phys.* B64 (1986) 189.
- [5] M.K. Wu, J.R. Asburn, C.J. Torng, P.H. Hor, R.L. Meng, L. Gao, Z.J. Huang, Y.O. Wang, C.W. Chu, *Phys. Rev. Lett.* 58 (1987) 908.
- [6] S.B.M. Hagstrom, C. Nardling, K. Seigbahn, *Z. Phys.* 178 (1964) 433.
- [7] U. Linder, H. Papp, *Appl. Surf. Sci.* 32 (1988) 75.
- [8] G. Moretti, G. Fierro, M. Lo Jacono, P. Porta, *Surf. Interface Anal.* 14 (1989) 325.
- [9] G. Moretti, S. De Rossi, G. Ferraris, *Appl. Surf. Sci.* 45 (1990) 341.
- [10] Y. Fukuda, T. Suzuki, M. Nagoshi, Y. Syono, K. Oh-ishi, M. Tachiki, *Solid State Commun.* 72 (1989) 1183.
- [11] W. Wang, T. Lu, Y. Gong, Y. Sun, *Surf. Sci.* 213 (1989) 303.
- [12] K.A. Babushkina, M.V. Dobrotvorskaya, N.A. Kasatkina, Y.B. Boltoratsky, V.B. Sobolev, S.V. Kuchienko, *Physica C*197 (1992) 299.
- [13] P. Steiner, V. Kinsinger, I. Sander, B. Seigwart, S. Hufner, C. Politis, R. Hoppe, H.P. Müller, *Z. Phys.* B67 (1987) 502.
- [14] F. Parmigiani, L. Depero, T. Minerva, J.B. Torrance, *J. Electron Spectr. Rel. Phenom.* 58 (1992) 315.
- [15] K. Allan, A. Champion, J. Zhou, J.B. Goodenough, *Phys. Rev.* B41 (1990) 11572.
- [16] K. Wandelt, *Surf. Sci. Rep.* 2 (1982) 1.
- [17] B.M.J. Smets, T.P.A. Lommen, *J. Non-Cryst. Solids* 46 (1981) 21.
- [18] X. Lu, H. Jain, W.C. Huang, *Phys. Chem. Glasses* 37 (1996) 201.
- [19] D.S. Goldman, *Phys. Chem. Glasses* 27 (1986) 128.
- [20] R. Gersch, W.M. Warmuth, H. Dutz, *J. Non-Cryst. Solids* 34 (1979) 127.
- [21] C.H. Hseih, H. Jain, A.C. Miller, E.I. Kamitsos, *J. Non-Cryst. Solids* 168 (1994) 132.
- [22] R.K. Brow, R.J. Kirkpatrick, G.L. Turner, *J. Am. Ceram. Soc.* 73 (1990) 2239.
- [23] N.F. Mott, E.A. Davis, *Electrical Processes in Non-Crystalline Materials* (Clarendon, Oxford, 1971).
- [24] M. Sayer, A. Mansingh, *Phys. Rev.* B6 (1972) 4629.

- [25] H.O Hooper, A.M. Graff, eds., *Amorphous Magnetism*, Proc. Int. Symposium on Amorphous Magnetism (Plenum, New York, 1973).
- [26] C.R. Banford, *Colour Generation and Control in Glass* (Elsevier Science, Amsterdam, 1977).
- [27] R.K. Brow, C.M. Arens, X. Yu, E. Day, *Phys. Chem. Glasses* 35 (1994) 132.
- [28] A. Mekki, D. Holland, C.F. McConville, M. Salim, *J. Non-Cryst. Solids* 208 (1996) 267.
- [29] E.E. Khawaja, Z. Hussain, M.S. Jazzar, O.B. Daboussi, *J. Non-Cryst. Solids* 93 (1987) 45.
- [30] M.T. Anthony, M.P. Seah, *Surf. Interface Anal.* 6 (1984) 95.
- [31] B.M.J. Smets, T.P.A. Lommen, *J. Am. Ceram. Soc.* 65 (1982) C–80.
- [32] L.F. Olfield, *Glass Technol.* 5 (1964) 41.
- [33] D.C. Frost, A. Ishitani, C.A. McDowell, *Molec. Phys.* 24 (1972) 861.
- [34] G. Schön, *Surf. Sci.* 35 (1973) 96.
- [35] K.S. Kim, *J. Electron Spectr. Rel. Phen.* 3 (1974) 217.
- [36] B. Wallbank, I.G. Main, C.E. Johnson, *J. Electron Spectr. Rel. Phenom.* 5 (1974) 259.
- [37] A. Proctor, P.M.A. Sherwood, *Anal. Chem.* 52 (1980) 2351.
- [38] B.M.J. Smets, D.M. Krol, *Phys. Chem. Glasses* 25 (1983) 113.
- [39] B.W. Veal, D.J. Lam, A.P. Paulikas, *J. Non-Cryst. Solids* 49 (1982) 309.